JOURNAL OF THE AMERICAN COLLEGE OF CARDIOLOGY VOL. 73, NO. 18, 2019

Myofibroblast Phenotype and Reversibility of Fibrosis in Patients With End-Stage Heart Failure

Chandan K. Nagaraju, MSc,[a] Emma L. Robinson, PhD,[a] Mouna Abdesselem, PhD,[a] Sander Trenson, MD,[a] Eef Dries, PhD,[a] Guillaume Gilbert, PhD,[a] Stefan Janssens, MD, PhD,[b] Johan Van Cleemput, MD, PhD,[b] Filip Rega, MD, PhD,[b] Bart Meyns, MD, PhD,[b] H. Llewelyn Roderick, PhD,[a] Ronald B. Driesen, PhD,[a] Karin R. Sipido, MD, PhD[a]

ABSTRACT

BACKGROUND Interstitial fibrosis is an important component of diastolic, and systolic, dysfunction in heart failure (HF) and depends on activation and differentiation of fibroblasts into myofibroblasts (MyoFb). Recent clinical evidence suggests that in late-stage HF, fibrosis is not reversible.

OBJECTIVES The study aims to examine the degree of differentiation of cardiac MyoFb in end-stage HF and the potential for their phenotypic reversibility.

METHODS Fibroblasts were isolated from the left ventricle of the explanted hearts of transplant recipients (ischemic and dilated cardiomyopathy), and from nonused donor hearts. Fibroblasts were maintained in culture without passaging for 4 or 8 days (treatment studies). Phenotyping included functional testing, immunostaining, and expression studies for markers of differentiation. These data were complemented with immunohistology and expression studies in tissue samples.

RESULTS Interstitial fibrosis with cross-linked collagen is prominent in HF hearts, with presence of activated MyoFbs. Tissue levels of transforming growth factor (TGF)-β1, lysyl oxidase, periostin, and osteopontin are elevated. Fibroblastic cells isolated from HF hearts are predominantly MyoFb, proliferative or nonproliferative, with mature α-smooth muscle actin stress fibers. HF MyoFb express high levels of profibrotic cytokines and the TGF-β1 pathway is activated. Inhibition of TGF-β1 receptor kinase in HF MyoFb promotes dedifferentiation of MyoFb with loss of α-smooth muscle actin and depolymerization of stress fibers, and reduces the expression of profibrotic genes and cytokines levels to non-HF levels.

CONCLUSION MyoFb in end-stage HF have a variable degree of differentiation and retain the capacity to return to a less activated state, validating the potential for developing antifibrotic therapy targeting MyoFb.
(J Am Coll Cardiol 2019;73:2267–82)

Fibrosis with excessive collagen deposition in the matrix is part of the remodeling process in heart disease, which substantially contributes to contractile dysfunction. Reducing fibrosis has become a major target in cardiovascular research (1), but fibrosis is also necessary for the repair process and scar formation after myocardial infarction (MI). This scar tissue is enriched in cross-linked collagen fibers. These are produced by myofibroblasts (MyoFb) and serve to provide strength and protection against rupture. However, interstitial fibrosis in the remote myocardium after MI, in hypertensive and in

Listen to this manuscript's audio summary by Editor-in-Chief Dr. Valentin Fuster on JACC.org.

From the [a]Department of Cardiovascular Sciences, KU Leuven, Leuven, Belgium; and the [b]Department of Cardiology and Department of Cardiac Surgery, University Hospitals Leuven, Leuven, Belgium. Support for the work was provided by the Fund for Scientific Research Flanders (G091815N to Dr. Sipido, FWO Odysseus grant 90663 to Dr. Roderick, and post-doctoral fellowships to Drs. Dries and Driesen), the Belgian Science Policy (IAP7/10, to Dr. Sipido), and the European Commission (MSCA-IF-2016-752824, to Dr. Abdesselem). Dr. Rega has received research funding from Medtronic; and has been a consultant to AtriCure and Liva Nova. All other authors have reported that they have no relationships relevant to the contents of this paper to disclose.

Manuscript received April 18, 2018; revised manuscript received January 24, 2019, accepted February 4, 2019.

ISSN 0735-1097 https://doi.org/10.1016/j.jacc.2019.02.049

ABBREVIATIONS AND ACRONYMS

DCM = dilated cardiomyopathy

dediff-MyoFb = dedifferentiated myofibroblast(s)

ECM = extracellular matrix

Fb = fibroblast(s)

HF = heart failure

ICM = ischemic cardiomyopathy

LV = left ventricle/ventricular

MI = myocardial infarction

MMP = matrix metalloproteinase

MyoFb = myofibroblast(s)

Non-HF = nonfailing heart(s)

non-p-MyoFb = non-proliferating myofibroblast(s)

p-MyoFb = proliferating myofibroblast(s)

TGF = transforming growth factor

TIMP = tissue inhibitor of matrix metalloproteinases

SMA = smooth muscle actin

cardiometabolic disease, is an important cause of diastolic dysfunction (2-5). Moreover, interstitial and patchy fibrosis seen in dilated cardiomyopathy (DCM) may interfere with conduction and facilitate arrhythmias (6).

SEE PAGE 2283

Interstitial fibrosis is part of an inflammatory process that causes fibroblasts (Fb), resident in the healthy heart, to differentiate into MyoFb during disease (7). Recruitment of mesenchymal cells further contributes to fibrosis (8,9). Fibroblast activation and differentiation are induced by mechanical cues from increased hemodynamic loading, and from cytokines and growth factors secreted by inflammatory cells and cardiac myocytes. These signals are reinforced by autocrine signaling (10,11). The increased matrix deposition by MyoFb is not static, but rather undergoes remodeling through the actions of matrix metalloproteinases (MMPs) and tissue inhibitor of matrix metalloproteinases (TIMPs), which are predominantly secreted by leukocytes and other nonmyocyte cells of the heart (12,13).

In experimental studies, modulation of transforming growth factor (TGF)-β signaling and other pathways reduced interstitial fibrosis and improved left ventricular (LV) function (14,15). Targeting GRK2 signaling pathways that are shared between myocytes and Fb had beneficial effects (16). Interventions targeting inflammation also reduced fibrosis (17).

Current clinical guidelines for the treatment of chronic heart failure (HF) do not include drugs specifically aimed at reversal of fibrosis but drugs targeting the renin-angiotensin-aldosterone system pathway can reduce fibrosis indirectly (18-20). Hemodynamic unloading following replacement of a stenotic aortic valve reduced fibrosis and improved cardiac function (21). In the failing human heart, hemodynamic unloading with assist devices partially restored heart function, with recovery of myocyte contractile capacity and partial reversal of some of the maladaptive myocyte molecular changes (22-24). However, a recent patient study also showed that in late-stage HF, unloading the ventricle did not reverse fibrosis (25).

This raises the question of whether in patients with advanced HF, MyoFb have become terminally differentiated and have lost the potential for recovery toward a quiescent fibroblast phenotype. Animal studies rarely reproduce the long-time course of human HF and thus cannot answer this question. In the present study, we therefore investigated the nature of collagen deposition and fibroblast phenotype in human end-stage HF and explored the potential for reversal of the MyoFb to a normal/healthy Fb phenotype. For this purpose, we used tissue samples obtained from explanted hearts taken at the time of heart transplantation (HF, both ischemic cardiomyopathy [ICM] and DCM), and samples from nonfailing hearts (Non-HF). In these human heart samples, we examine fibrosis and Fb phenotypes in situ, and in cells in short-term culture. We use an inhibitor of the TGF-β1 pathway to test the potential for phenotype reversibility.

MATERIAL AND METHODS

At the time of explantation, hearts were collected and placed in cardioplegic solution (n = 17 for Non-HF and n = 27 for HF). Tissue samples were taken from the LV anterior and posterior wall, avoiding post-MI scar tissue in HF. Samples for isolation of Fb were processed immediately, whereas samples for histology and molecular analysis were either fixed or snap-frozen in liquid nitrogen and stored at −80°C for later analysis. Non-HF tissue samples were obtained from nonfailing donor hearts that were considered unsuitable for heart transplantation. Online Table 1 provides information on the patient population from which HF and non-HF samples were obtained. The study protocol was approved by the ethical committee of UZ Leuven (S58824), conformed to the Helsinki declaration, and was conducted in accordance with the prevailing national and European Union regulations on the use of human tissues. A detailed methods description is provided in the Online Appendix, including all primers of mRNA studies (Online Table 2) and a flow chart of cell processing and experimental design (Online Figure 1).

RESULTS

INCREASED INTERSTITIAL FIBROSIS, COLLAGEN CROSS-LINKING, AND ACTIVATED MyoFb IN HF. We quantified collagen with Sirius red staining in tissue sections and used polarization microscopy to identify cross-linking (Online Figures 2A and 2B). The fractional area with fibrosis was 4 times higher in HF hearts compared with Non-HF. Both thick cross-linked collagen fibers, mostly collagen I, and non-crossed-linked thin collagen fibers, mostly type III, were more abundant (Online Figure 2C). Increased mRNA levels of collagen type I and type III (Online

FIGURE 1 HF LV Interstitial Fibrosis, Fb Differentiation and Proliferation In Situ

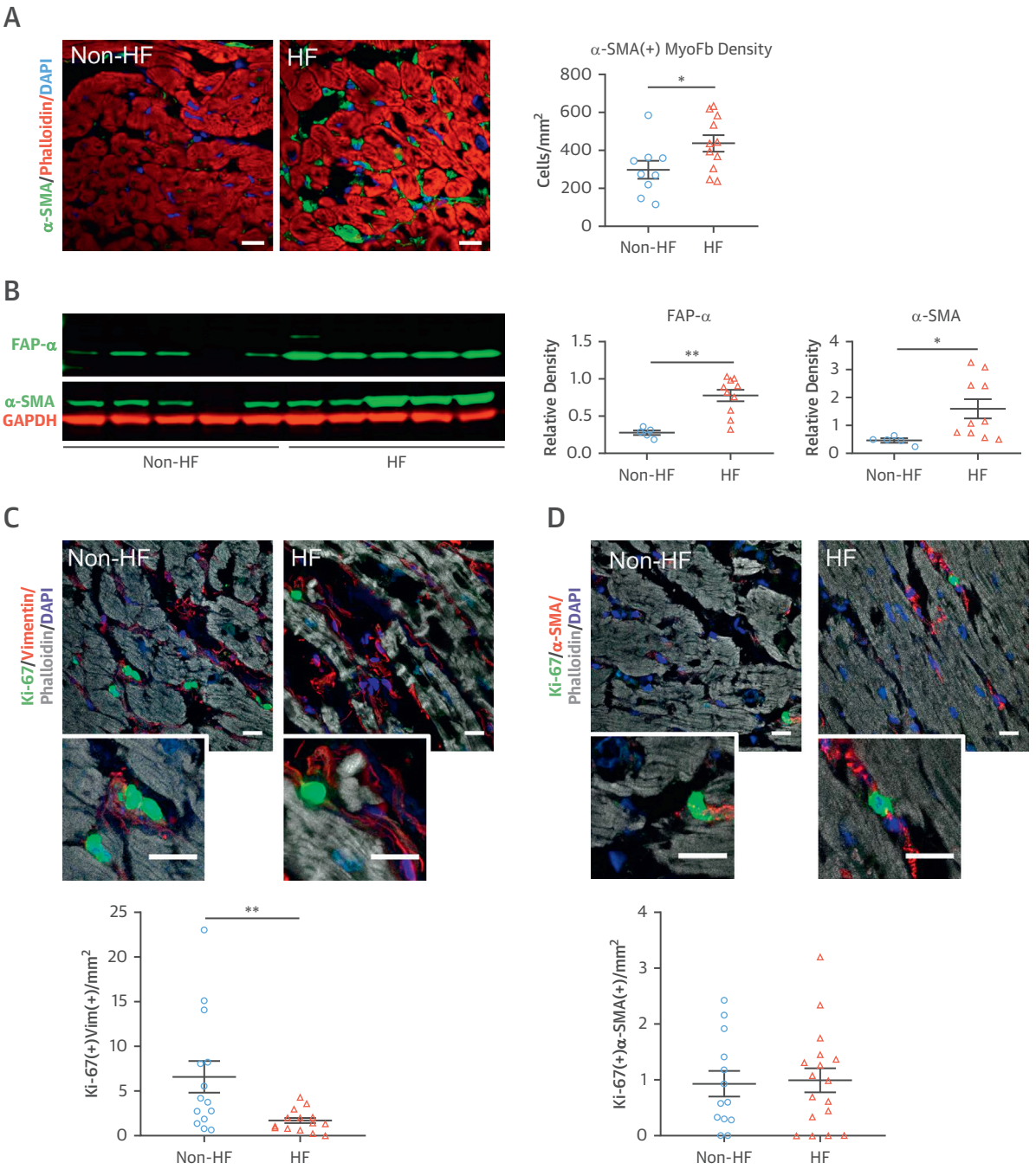

(A) Analysis of density of MyoFb cells based on α-SMA staining. n = 9 for Non-HF, n = 11 for HF. **(B)** Immunoblot analysis of protein expression for markers of MyoFb, FAP-α (88 kDa), and α-SMA (42 kDa), normalized to GAPDH (37 kDa), in tissue homogenates. n = 5 for Non-HF, n = 10 for HF. **(C)** Identification and analysis of cells, both Ki-67-positive and vimentin-positive, representing predominantly fibroblastic cells. **(D)** Identification and analysis of proliferating α-SMA–positive MyoFb. n = 14 for Non-HF, n = 17 for HF; for each heart, an area of 4.3 mm^2 was analyzed. **Scale bars** represent 20 μm. *$p < 0.05$, **$p < 0.01$ (Student's *t*-test, 2-tailed, unpaired). DAPI = 4′,6-diamidino-2-phenylindole; FAP-α = fibroblast activation protein alpha; Fb = fibroblasts; GADPH = glyceraldehyde 3-phosphate dehydrogenase; HF = heart failure; LV = left ventricular; MyoFb = myofibroblasts; Non-HF = nonused donor hearts; SMA = smooth muscle actin.

FIGURE 2 Advanced Differentiation of Fb Isolated From Failing Human Hearts

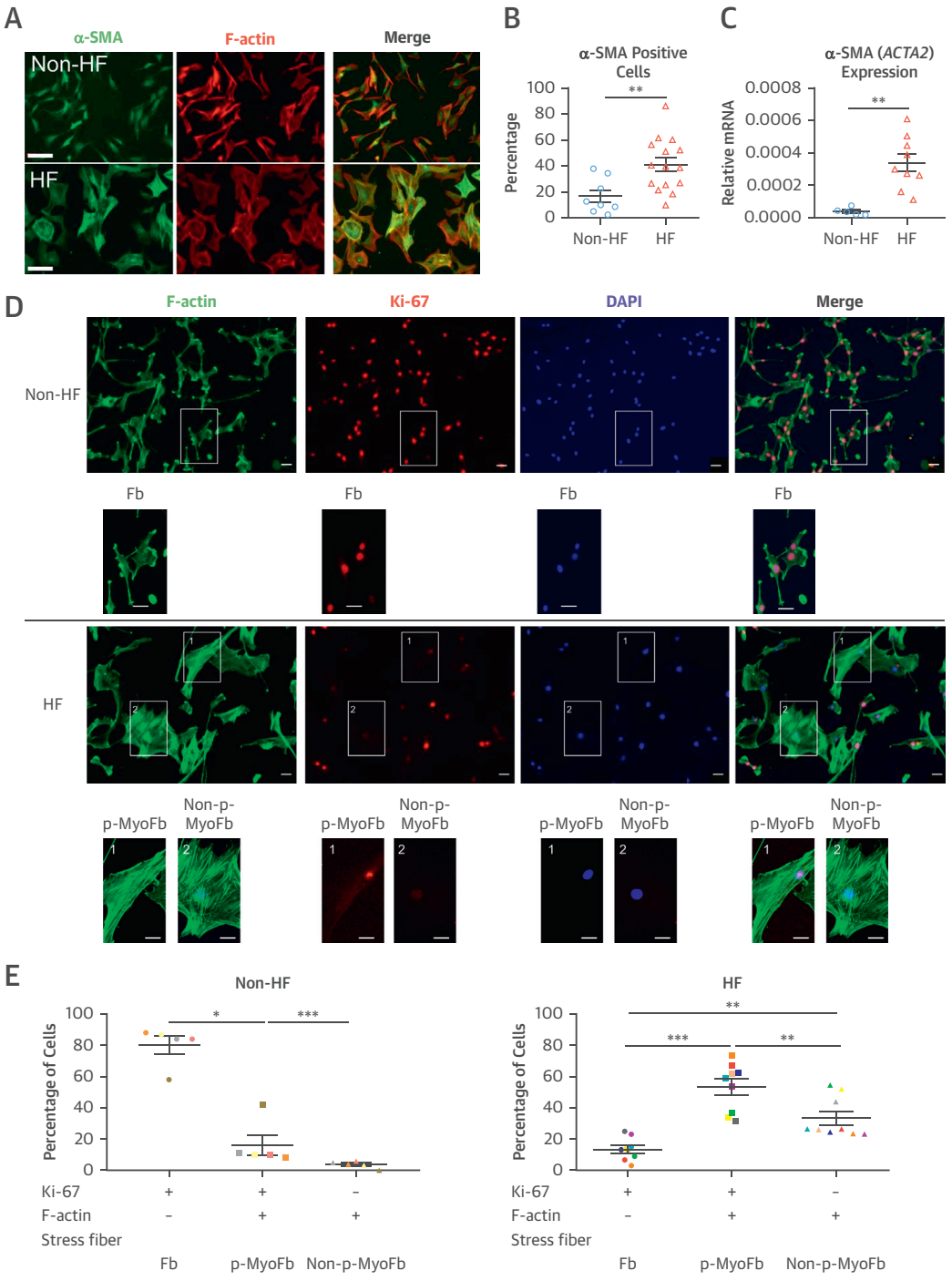

(A) Overlay of images of cells stained for F-actin **(red)** and α-SMA **(green)**, at 4 days after isolation. **(B)** Quantification of α-SMA–positive cells as percentage of all cells. n = 7 for Non-HF, n = 15 for HF. **(C)** α-SMA (*ACTA2*) gene expression by RT-qPCR. n = 5 for Non-HF, n = 9 for HF. **(D)** Images of immunofluorescent staining of the phenotype marker F-actin **(green)**, the proliferation marker Ki-67 **(red)**, and nucleus DAPI **(blue)**. **Scale bars** represent 20 μm. **(E)** Quantification of phenotypes: Fb, proliferating and nonproliferating MyoFb. n = 5 for Non-HF, n = 9 for HF. **Dot colors** identify data from the same heart. *p < 0.05, **p < 0.01, ***p < 0.001 (Student's *t*-test, 2-tailed, unpaired for **B and C**, and 1-way ANOVA with Bonferroni post hoc test for **E**). ANOVA = analysis of variance; p-MyoFb = proliferating myofibroblasts; RT-qPCR = quantitative reverse transcription polymerase chain reaction; other abbreviations as in Figure 1.

Figure 2D) support the imaging data. There was a positive correlation between increased fibrosis measured by Sirius red staining and collagen type I, but not collagen type III (Online Figure 2E and 2F).

Using Fb/MyoFb markers, we assessed Fb and MyoFb cell density in situ. Vimentin-positive cells, including all fibroblast types, were more numerous in HF hearts than in Non-HF (Online Figure 3). More specifically, the density of (α-smooth muscle actin [SMA]-positive) MyoFb was higher in HF hearts than in Non-HF (**Figure 1A**). The protein expression of fibroblast activation protein alpha (FAP-α), a specific marker of cardiac MyoFb, and of α-SMA (**Figure 1B**), was also higher in HF. To identify proliferation in situ, we used Ki-67 nuclear staining (DAPI and Ki-67) as a marker. We quantified colocalization with vimentin or α-SMA staining around the Ki-67–positive nucleus to indicate all fibroblastic cells or MyoFb, respectively (**Figures 1C and 1D**). The density of Ki-67–positive fibroblastic cells was generally low, and higher in Non-HF than in HF hearts. The density of proliferating MyoFb was even lower at 1 cell/mm^2 and not different between HF hearts and Non-HF.

Collectively, the data indicate that in situ, the fibroblastic cells in end-stage HF are mostly MyoFb, of which some remain proliferative.

FB ISOLATED FROM HF HEARTS ARE MOSTLY DIFFERENTIATED MyoFb. To characterize the Fb population, we isolated cells and maintained them in short-term culture (4 days, no passaging) for subsequent phenotyping. We confirmed high proportion of the cultures (Online Figure 4). Cells from HF hearts had a high proportion of differentiated MyoFb with F-actin stress fibers (red color) decorated with α-SMA (green color) (**Figures 2A and 2B**). Reverse transcription quantitative polymerase chain reaction (RT-qPCR) confirmed 8-fold higher mRNA levels of α-SMA *(ACTA2)* in HF cells (**Figure 2C**). The degree of in vitro differentiation significantly correlated with increased fibrosis measured in situ (Online Figure 5). The fraction of α-SMA–positive cells was not different between ICM and DCM (Online Figure 6).

To define more specific phenotypes, we performed a double staining for Ki-67 as a nuclear marker for proliferation, and F-actin stress fibers as a marker for MyoFb differentiation (**Figure 2D**). Cells were classified as either Fb (Ki-67 positive and stress fiber F-actin negative), proliferating MyoFb (p-MyoFb) (Ki-67 positive and stress fiber F-actin positive), and non-proliferating MyoFb (non-p-MyoFb) (Ki-67 negative and stress fiber F-actin positive) (**Figure 2E**). Quantification of these stained samples confirmed that in Non-HF, most cells were nondifferentiated and proliferating Fb, whereas in HF, MyoFb prevailed, but with 2 different subtypes, proliferative (55%) and nonproliferative MyoFb (37%). This analysis of cellular phenotypes indicates that in fibroblasts isolated from HF hearts, MyoFb are the predominant cell type, and a substantial fraction of these MyoFb retain the capacity for proliferation.

INCREASED GENE EXPRESSION FOR MATRIX REMODELING IN HF MyoFb. To assess the capacity of HF MyoFb for matrix remodeling, we measured related gene expression profiles by RT-qPCR analysis of mRNA prepared from cell lysates. Compared with Non-HF, MyoFb from HF hearts had increased expression of profibrotic genes such as those for monocyte chemo attractant protein (MCP1/CCL2), connective tissue growth factor (CTGF), interleukin (IL)-4, and eotaxin (CCL11) (**Figure 3A**). Furthermore, they had higher expression levels of collagen type I (COL1A2) and collagen type III (COL3A1) along with lysyl oxidase (LOX), which promotes collagen cross-linking (**Figure 3B**). Expression of activators of LOX such as periostin (POSTN) and osteopontin (OPN) was also increased in HF (**Figure 3C**).

For proteins related to turnover of matrix, we detected elevated mRNA expression of MMP3, MMP9, and TIMP1, TIMP2, and TIMP3 in cells isolated from HF hearts (**Figure 3D**).

The TGF-β signaling pathway for Fb differentiation was significantly activated in HF (**Figure 3E**). mRNA expression levels of TGF-β receptor 1 and 2, which form the ALK-5 complex, as well as members of the downstream SMAD (SMAD2, SMAD3, and SMAD4) signaling pathway, were markedly increased. Biomechanical stress can activate myocardin-related transcription factors (MRTF-A/B), independent of TGF-β signaling, and promote Fb differentiation (26), but expression of MRTFs between HF and Non-HF was not different (**Figure 3F**).

This indicates that MyoFb isolated from HF hearts have a gene expression profile consistent with increased production and turnover of matricellular proteins, and with activation of TGF-β signaling.

PROFIBROTIC SIGNALING AND INFLAMMATION IN HF. We investigated whether the findings in isolated cells correspond to activation of Fb in the heart in situ and examined the key components of TGF-β signaling pathway in tissue samples. Immunofluorescent staining of TGF-β1 in tissue sections (**Figure 4A**) was higher in HF hearts compared with Non-HF, which was supported by similar findings from immunoblotting of tissue homogenates (**Figure 4A**). Activation

FIGURE 3 Enhanced Expression of Fibrosis-Related Genes in Cells Isolated From HF Hearts

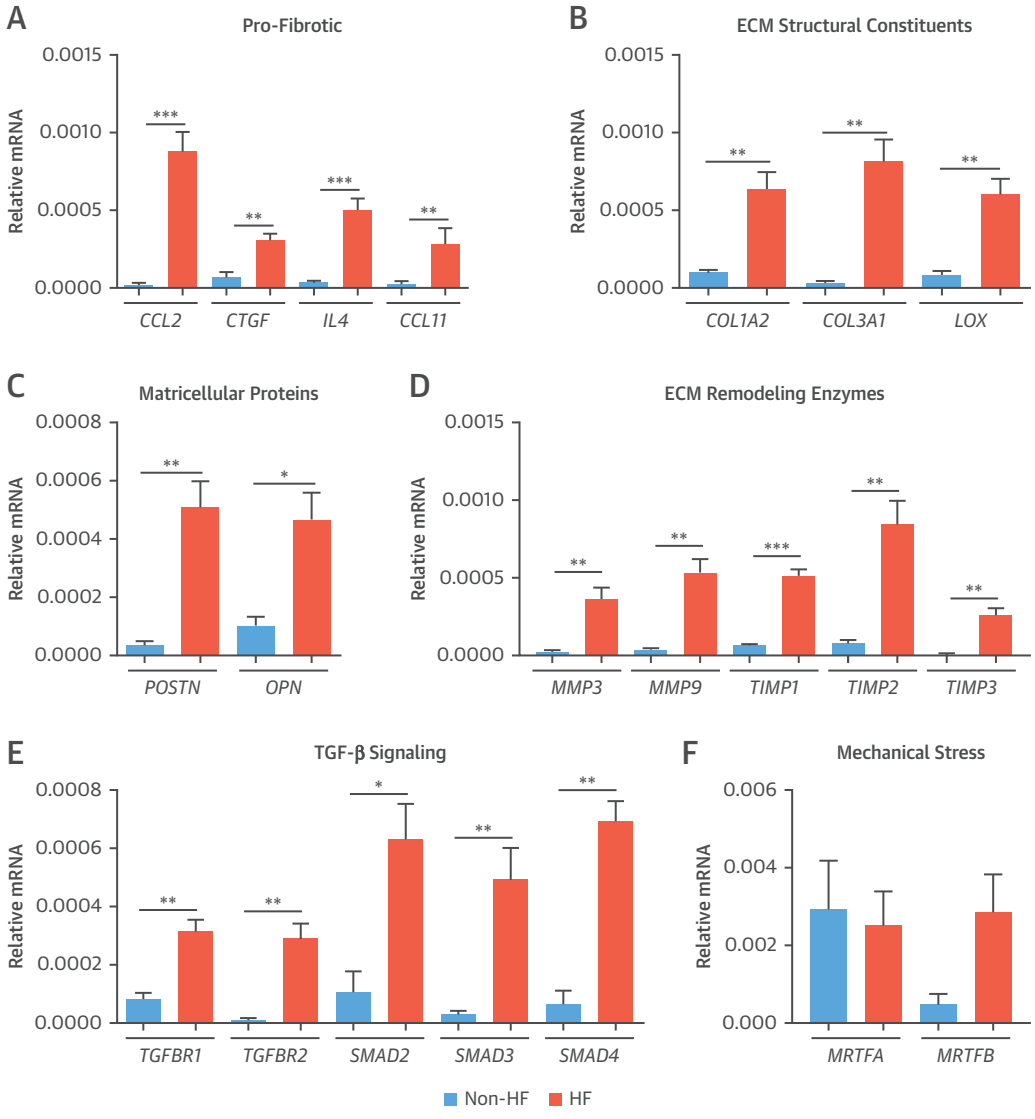

Quantification of gene expression using RT-qPCR after 4-day culture of cells isolated from HF hearts and Non-HF. **(A)** Profibrotic genes *CCL2*, *CTGF*, *IL-4*, and *CCL11*. **(B)** Extracellular matrix structural constituent genes for collagen production *COL1A2*, *COL3A1*, and *LOX*. **(C)** Genes for the matricellular proteins POSTN and OPN. **(D)** Genes for the enzymes involved in collagen metabolism: *MMP3*, *MMP9*, *TIMP1*, *TIMP2*, and *TIMP3*. **(E)** TGF-β signaling pathway genes *TGFBR1*, *TGFBR2*, *SMAD2*, *SMAD3*, and *SMAD4*. **(F)** Genes activated by mechanical stress, *MRTFA* and *MRTFB* (n = 5 for Non-HF, n = 9 for HF hearts). *p < 0.05, **p < 0.01, ***p < 0.001 (Student's *t*-test, 2-tailed, unpaired). ECM = extracellular matrix; OPN = osteopontin; POSTN = periostin; TGF = transforming growth factor.

of TGF-β1 in HF hearts was further supported by high levels of phosphorylation of its downstream targets SMAD2 and SMAD3 (**Figure 4B**). TGF-β1 expression in tissue moderately correlated with interstitial fibrosis (Online Figure 7A).

Because collagen type I is highly cross-linked in HF hearts, we examined protein expression of components of the pathway involved in LOX activation. Precursors of LOX (pre-LOX), mature LOX, and periostin, which leads to activation of LOX (27), were significantly up-regulated in HF hearts (**Figure 4C**) and correlated with collagen type I (Online Figure 7B). Because inflammatory cells are a source of cytokines, we quantified tissue-associated macrophages ($CD68^+$ cells) and saw a higher number of macrophages in HF hearts compared with Non-HF (**Figure 4D**).

FIGURE 4 Signaling for Differentiation, Collagen Cross-Linking, and Inflammation In Situ

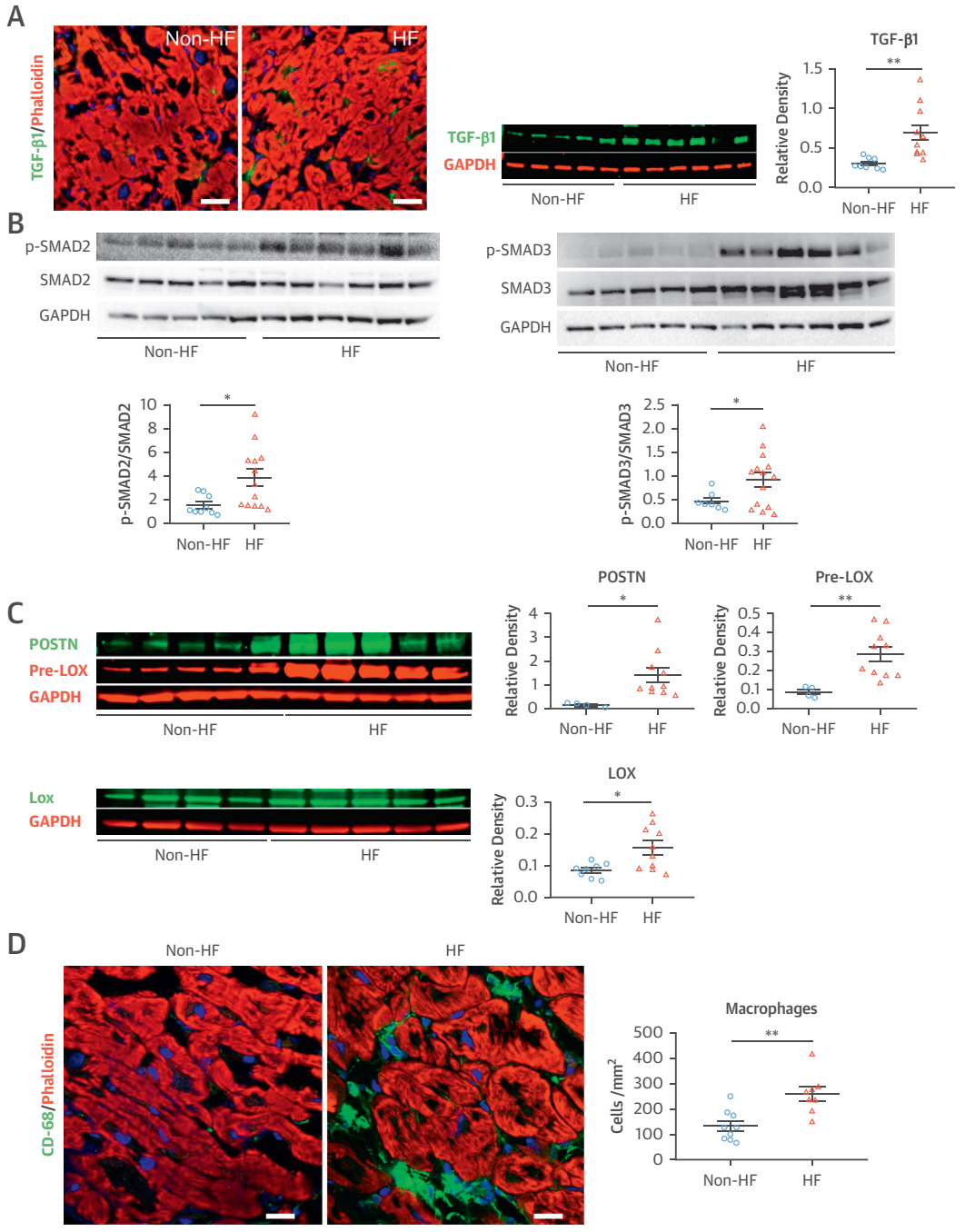

(A) TGF-β1 presence in tissue samples from HF hearts and Non-HF shown in immunofluorescence staining and immunoblot of homogenates. n = 9 for Non-HF, n = 11 for HF. **(B)** Activation of SMAD2 (60 kDa), SMAD3 (52 kDa), and reference GAPDH (37 kDa) in tissue homogenates from HF hearts and Non-HF shown by Western blot. n = 9 for Non-HF, n = 13 for HF in SMAD2 blot; n = 8 for Non-HF, n = 14 for HF in SMAD3 blot. **(C)** Protein expression using immunoblot for POSTN (93 kDa), pre-LOX (50 kDa), mature LOX (35 kDa), and GAPDH (37 kDa) in tissue samples. n = 5 for Non-HF, n = 10 for HF in POSTN and pre-LOX blots; n = 8 for Non-HF, n = 10 for HF in LOX blot. **(D)** Immunofluorescence staining and analysis of CD-68–positive macrophages. (n = 9 for Non-HF, n = 8 for HF in **D**). *p < 0.05, **p < 0.01 (Student's *t*-test, 2-tailed, unpaired). LOX = lysyl oxidase; other abbreviations as in Figures 1, 2, and 3.

Together, these data indicate that proinflammatory signals and matrix remodeling remain active in end-stage HF.

BLOCKING OF TGF-β1 SIGNALING REVERSES THE MyoFb PHENOTYPE. To test for reversibility of the MyoFb phenotype, we treated HF cells with SD-208, a specific TGF-β receptor-I (TGF-β-RI) kinase inhibitor, starting at day 4 and quantitated markers of de-differentiation (Online Figure 1). The cells were maintained under treatment for an additional 4 days and phenotyped at day 8; Non-HF at day 8 was included as reference. The levels of phosphorylated SMAD2 were significantly decreased under treatment, confirming the inhibition of TGF-β signaling (Online Figure 8A).

Comparing treated with nontreated HF at the same time point of day 8, cells with α-SMA–positive stress fibers were more scarce (32% vs. 65% in nontreated) (**Figures 5A and 5B**). Similarly, α-SMA mRNA *(ACTA2)* expression levels after SD-208 treatment were 2-fold lower than in nontreated HF (**Figure 5C**), as were the protein levels (Online Figure 8B). Further evidence for the loss of the MyoFb phenotype comes from measuring the capacity of the cells to contract the surrounding extracellular matrix (ECM) when embedded in a 3-dimensional floating collagen gel (**Figure 5D**). Cells derived from HF hearts led to a larger reduction in collagen gel diameter (30%) compared with Non-HF; when HF cells were treated with SD-208, collagen contraction was reduced to levels similar to that in the Non-HF gels (**Figure 5E**). Of note, collagen contraction is a multifactorial process, not only dependent on α-SMA expression in MyoFb, but also on loss of cells, organization of the network, and other elements (28).

In a different experiment, we compared gene expression in HF cells at day 8 to the initial phenotype at day 4. mRNA levels of collagen type I, type III, and α-SMA were similar to day 4 after treatment with SD-208 (**Figures 5F to 5H**).

The aforementioned data support loss of MyoFb phenotype following SD-208 treatment but do not document dedifferentiation directly. We used confocal imaging and quadruple staining for more detailed phenotyping (**Figure 6A**). Cells were classified as Fb (no stress fibers, positive for proliferation marker Ki-67), proto-MyoFb (actin stress fibers, but no α-SMA), and p-MyoFb and non-p-MyoFb (α-SMA and F-actin stress fibers, with or without Ki-67 staining). We identified dedifferentiated MyoFb (dediff-MyoFb) by the loss of organization and the depolymerization of stress fibers with presence of aggregates: of α-SMA only or of both α-SMA and F-actin. Quantification of these phenotypes in treated and nontreated HF cell cultures is shown in **Figure 6B**. Compared with day 4, nontreated cultures at day 8 had an increase in MyoFb and a decrease in Fb, whereas dediff-MyoFb were very rare at either time point. With SD-208, dediff-MyoFb accounted for 26% of all cells, and the fraction of mature MyoFb was much smaller than in nontreated HF, as well as in HF on day 4. The SD-208 treatment also prevented further differentiation with a relative increase of Fb. Of note, overall cell density increased between day 4 and day 8 in treated and nontreated cultures (**Figure 6C**).

To further document the process of dedifferentiation and depolymerization at the level of individual cells, we tracked stress-fiber fate in individual cells after green fluorescent protein–labeling actin stress fibers using Lifeact (29) (**Figure 7**). With SD-208, loss of organized fibers and formation of aggregates can be observed in a single cell during repeated imaging. In nontreated cultures, cells can preserve fully organized stress-fibers (Online Figure 9). Notably, apoptosis in treated HF MyoFb remained low (Online Figure 10).

Together, these data provide evidence for the potential for true reversal of the MyoFb phenotype in HF.

GENE EXPRESSION IN DEDIFFERENTIATED HF MyoFb RESEMBLES NON-HF. In matched SD-208–treated samples, we examined the gene expression profile. Treatment with SD-208 led to lower expression levels of profibrotic genes *CCL2*, *CTGF*, *IL4*, and *CCL11* (**Figure 8A**). This was also the case for genes for ECM structural constituents *COL1A2*, *COL3A1*, and, to a lesser extent, *LOX* (**Figure 8B**), matricellular proteins *POSTN* (but less so for *OPN*) (**Figure 8C**), and ECM remodeling enzymes *MMP3*, *MMP9*, *TIMP1*, *TIMP2*, and *TIMP3* (**Figure 8D**) compared with the nontreated group. An analogue reduction in gene expression was found for the members of the TGF-β signaling pathway (**Figure 8E**) including *TGFBR1*, *TGFBR2*, *SMAD2*, *SMAD3*, and *SMAD4*, consistent with a less-differentiated phenotype. Treatment had no effect on the expression level of MRTFs in Non-HF or HF hearts (**Figure 8F**). In general, the gene expression pattern of treated cells from HF was not different from that of Non-HF except for *CCL11* and *LOX*.

DISCUSSION

The main findings of the present study are that: 1) the Fb/MyoFb population in the LV of the end-stage failing heart is heterogeneous in nature; and 2) the HF MyoFb have the potential for phenotype reversibility (**Central Illustration**).

FIGURE 5 Inhibition of TGF-β Signaling Promotes Dedifferentiation of MyoFb From HF Hearts

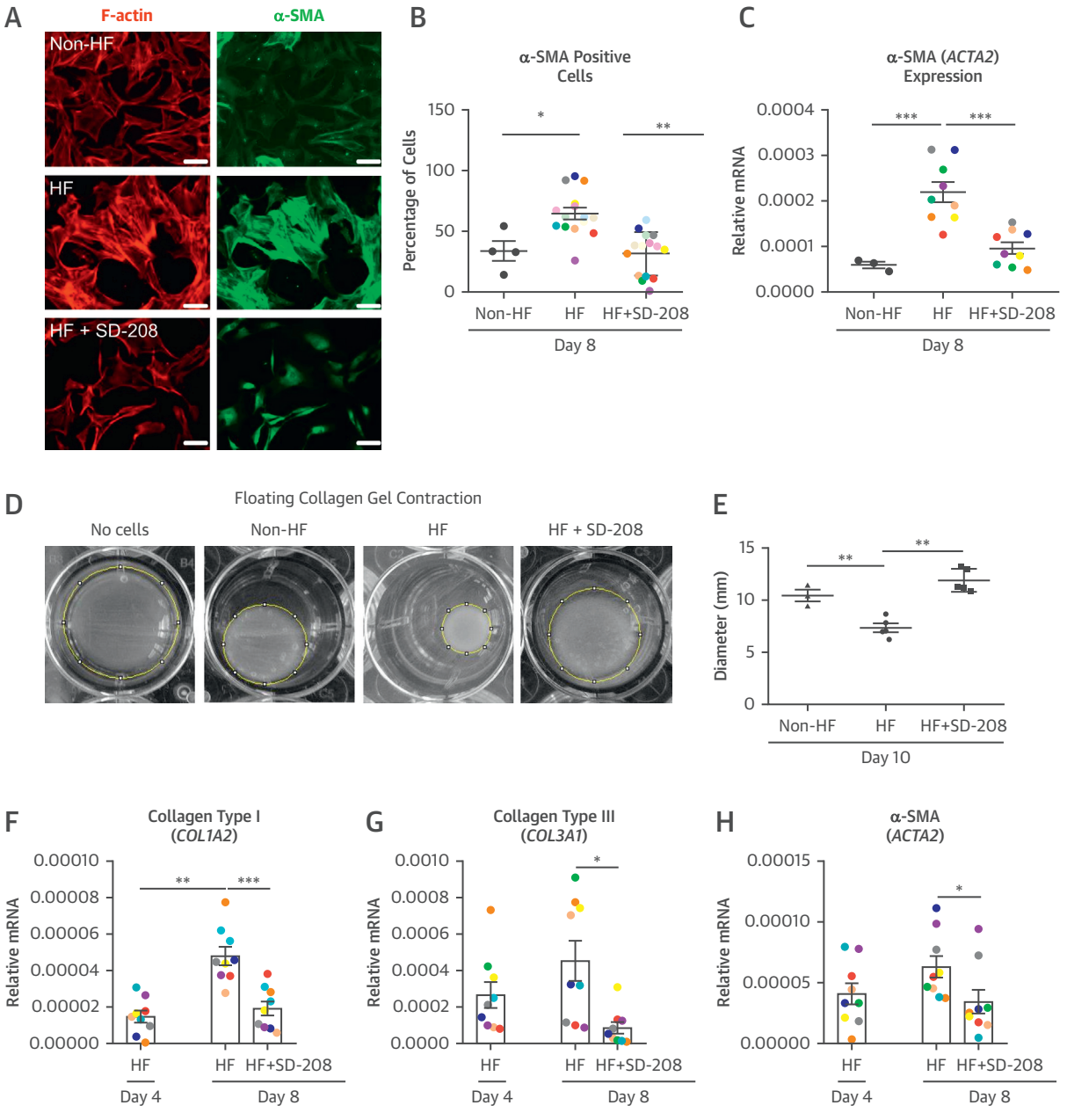

HF MyoFb were treated with SD-208 (3 μmol/l), and compared with nontreated HF MyoFb and cells from Non-HF. All cells were cultured for an additional 4 days after the first 4-day culture period. **(A)** Overlay of confocal fluorescent images of cells stained for F-actin **(red)** and α-SMA **(green)**. **(B)** Quantification of α-SMA–positive cells as a percentage of all cells. n = 4 for Non-HF, n = 15 for HF. **Dot colors** identify data from the same heart. **(C)** Quantification of α-SMA expression by RT-qPCR. n = 3 for Non-HF, n = 9 for HF. **(D)** Representative images of contraction of 3-dimensional rings by the embedded cells. **(E)** Analysis of the collagen gel diameter after 2 days in embedded collagen gel. n = 3 for Non-HF, n = 5 for HF. Quantification by RT-qPCR of collagen type I **(F)**, collagen type II **(G)**, and α-SMA **(H)**. n = 9 for HF. **Dot colors** identify data from the same heart. *$p < 0.05$, **$p < 0.01$, ***$p < 0.001$ (1-way ANOVA with Bonferroni post hoc test). Abbreviations as in Figures 1 and 2.

FIBROSIS AND MyoFb POPULATIONS IN END-STAGE HF. Cardiac fibrosis is a disease process, and only limited amounts of fibrillar collagen are present in the normal LV myocardium. Consistent with previous studies (30,31), we see a significant increase in interstitial fibrosis, collagen quantity, and cross-linking in end-stage HF. Almost all collagen is either type I or III, because the sum of both fractions corresponds

FIGURE 6 Phenotyping of Fb, MyoFb, and Dedifferentiated MyoFb in HF

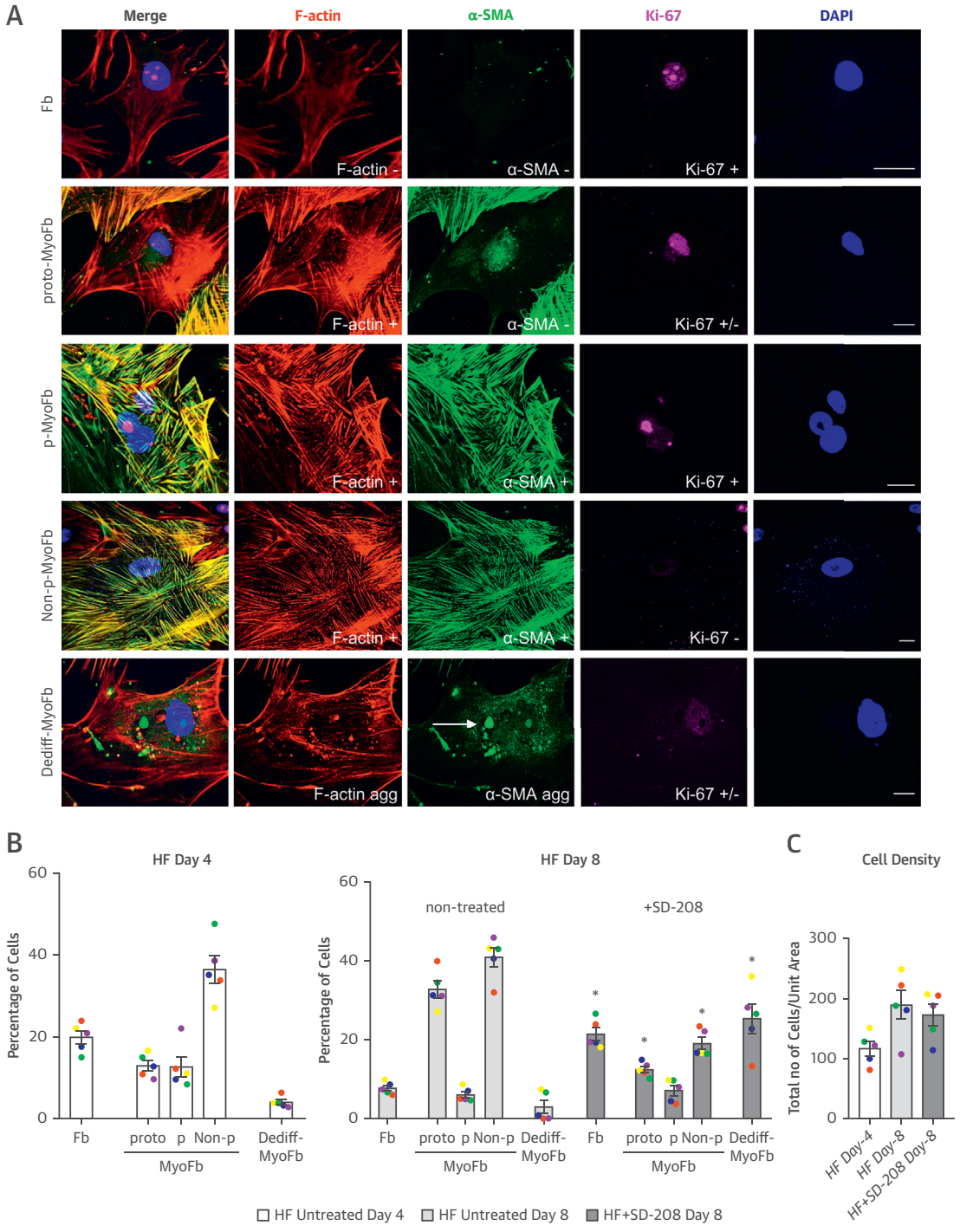

(A) Overlay and individual fluorescence channels of confocal images of cells stained for F-actin **(red)**, α-SMA **(green)**, DAPI **(blue)**, and Ki-67 **(pink)**. **(B)** Cells were classified as Fb (F-actin −, α-SMA −, Ki-67 +); proto-MyoFb (F-actin +, α-SMA −, Ki-67 +/−); proliferating MyoFb (F-actin +, α-SMA +, Ki-67 +); nonproliferating MyoFb (F-actin +, α-SMA +, Ki-67 −); dedifferentiated MyoFb (loss of stress fibers, with F-actin aggregates and/or α-SMA aggregates, Ki-67 +/−). Cells that were F-actin −, α-SMA −, and Ki-67 −, were not classified; their percentage was 14 ± 3% at day 4, 10 ± 2% at day 8, and 15 ± 3% for day 8 with SD-208. n = 5 for HF. **Dot colors** identify data from the same heart. *$p < 0.001$. **(C)** Cell density in treated and untreated HF MyoFb, counted per field of view (4.3 mm^2). (1-way ANOVA with Bonferroni post hoc test). Scale bar represents 20 μm. + = positive; − = negative; other abbreviations as in Figures 1 and 2.

closely to the fraction measured by Sirius Red staining. There was one exception in a DCM sample with a very high fraction of Sirius Red staining exceeding the sum of type I and type III, indicating the presence of other types of collagen or matricellular proteins. The fraction of collagen types was irrespective of the original etiology (Online Figures 11A and 11B). This contrasts with findings of an earlier study reporting that end-stage DCM was associated with loss of collagen type I (32). Although we did not see differences in the level of fibrosis and collagen subtypes, we found a higher level of LOX and periostin in DCM than in ICM patients (Online Figures 11C and 11D).

Both the data from in vitro culture and from in situ staining suggest that in HF, there is a heterogeneous population of fibroblastic cells. MyoFb are the most prominent cell type, and a small number of undifferentiated Fb remain present. The large fraction of differentiated MyoFb in vitro cannot be ascribed to the culturing process because in samples from Non-HF, more than 80% of cells were nondifferentiated. Of note, a substantial fraction of MyoFb isolated from HF hearts retained the potential for proliferation. Quantitatively, these data cannot be extrapolated directly to the in vivo situation. On one hand, in vitro culture conditions promote proliferation, as is also seen in the Non-HF Fb, and would lead to overestimation. On the other hand, capturing mitotic events or cell division in situ using immunostaining of small samples is challenging and may underestimate level of proliferation. Nevertheless, the in situ data support the notion that at least a fraction of MyoFb has not reached an end stage of differentiation. Collectively, these data indicate that in end-stage HF, the population of fibroblastic cells is heterogeneous, contrasting with a more homogeneous population of Fb in Non-HF.

The presence of cardiac macrophages is likely to play a role in maintaining and modulating Fb activation. These data also indicate that even in end-stage HF of patients under optimal therapy, inflammation still contributes to cardiac remodeling and functional phenotype (33).

The predominance of MyoFb in HF corresponds to high levels of TGF-β1. The latter can be released by the MyoFb (themselves) or the hypertrophied cardiac myocytes, or stored in the ECM as latent TGF-β1. Activation of the TGF-β1 signaling pathway was clear in both the isolated cell cultures, as well as within the native tissue samples, supporting an important role of the TGF-β signaling pathway in Fb differentiation and matrix remodeling. Yet, the activation of this pathway was higher in DCM than ICM (Online Figure 11E), suggestive of differences that depend on the HF etiology. Inflammation could be more pronounced, and/or the wall thinning in DCM may cause a higher wall stress that could explain some of the differences in activation of the TGF-β signaling pathway. Yet, MRTF, a transcription factor dependent on mechanical stress, was not differently expressed. This requires further investigation.

REVERSIBILITY OF MyoFb PHENOTYPE. The present data indicate that even in end-stage HF, MyoFb retain plasticity. Treatment of HF MyoFb with SD-208 silenced the profibrotic gene and matrix remodeling program. In particular, inhibition of the TGF-β1 signaling pathway reduced expression of LOX and its activators periostin and osteopontin. Direct evidence for the subsequent MyoFb dedifferentiation is the depolymerization of stress fibers with loss of stress fiber organization and contractile capability.

Although the data indicate reversibility in vitro of MyoFb, they do not address fibrosis reversibility. Experimental studies targeting MyoFb differentiation have shown some success (16,34), but translation to the clinical situation will require further research. Farris et al. (25) reported that cardiac unloading reduced fibroblast-specific collagen expression, but not the degree of fibrosis. Of note, MMP inhibition in the PREMIER (Prevention of Myocardial Infarction Early Remodeling) clinical trial (35) did not ameliorate post-MI remodeling, indicating more sophisticated strategies will be needed. Our data support the notion that the MyoFb retain plasticity, but there may be additional requirements to ensure turnover of the matrix and reduce collagen depositions.

The data also do not address whether in ICM, scar tissue would be affected or whether the risk for rupture would be increased. In the preclinical study of Travers et al. (16), treatment of mice was started 1 week after MI, and the overall collagen fraction was reduced, but this may have been related to myocyte protection, as well as to an effect on Fb in scar formation. Earlier studies on MI reported that inhibition of TGF-β1 1 week before MI or just after MI had a detrimental effect and increased mortality (36,37). In an ideal therapeutic strategy, MyoFb in scar tissue should be protected. In a previous study of highly differentiated non-p-MyoFb from rat heart, SD-208 inhibition of TGF-β1 had no effect (38). Whether such differences exist in humans remains to be evaluated.

The data in the present study are a proof of concept for potential reversibility of the MyoFb phenotype in late HF, but do not advocate for TGF-β inhibition, which has many side effects. Preclinical studies have identified signaling molecules downstream from the TGF-β1 receptor as possible targets (39–42). In mice

FIGURE 7 Live Cell Tracking of Dedifferentiation Process

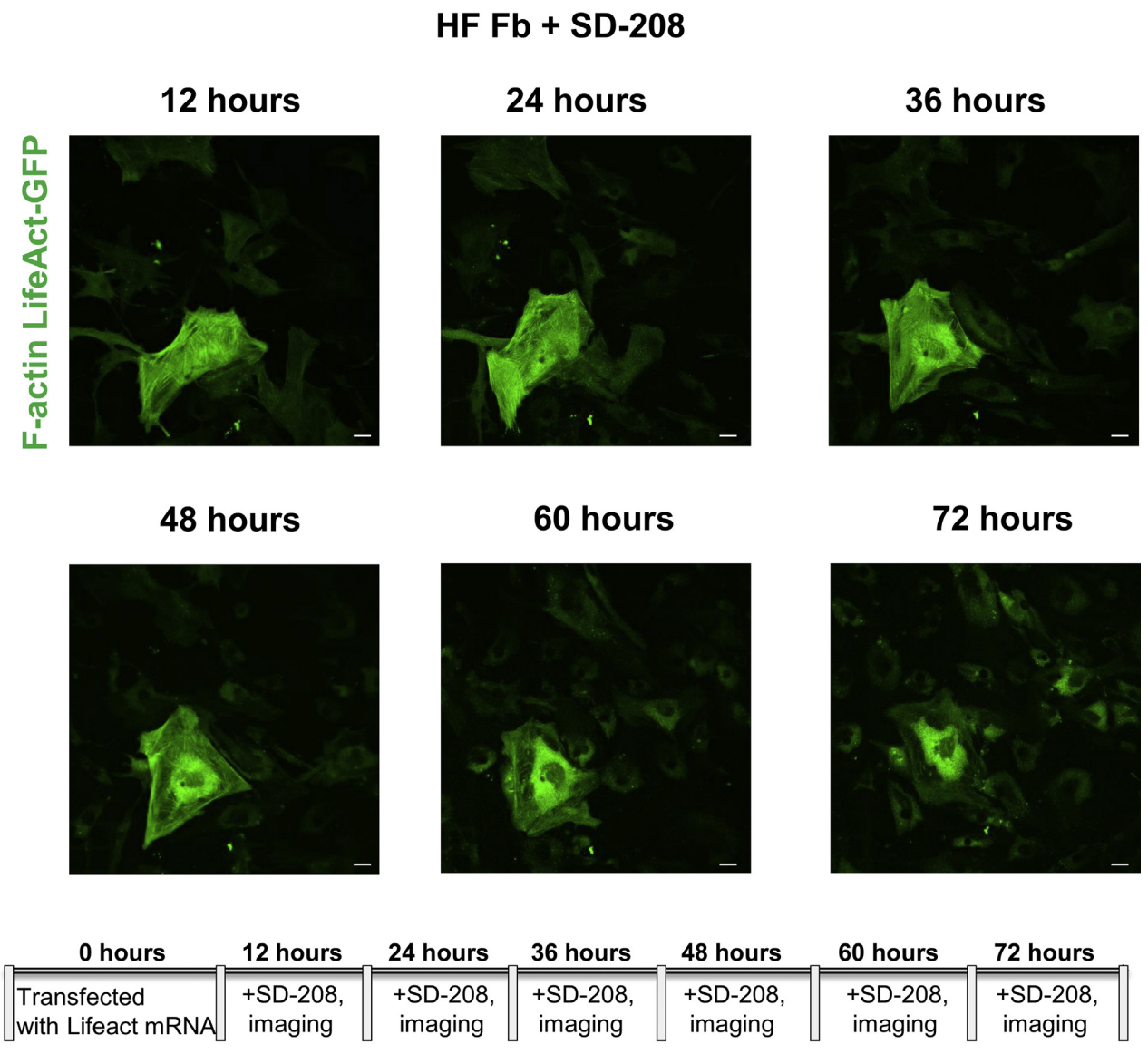

HF MyoFb were transfected with Lifeact-GFP mRNA on day 4. After labelling, SD-208 was added, and the cells were imaged by confocal microscopy every 12 h. A grid was used to track individual cells. Images are from the same cell over the time course shown. **Scale bar** represents 40 μm. GFP = green fluorescent protein; other abbreviations as in Figure 1.

with pressure-overload-induced interstitial fibrosis, overexpression of CCN5 interfered with TGF-β signaling, enhanced MyoFb apoptosis, and reduced established fibrosis (43). Recent approaches using unbiased screening in preclinical models pave the way for further studies in human tissues and eventual translation (44,45).

Fb differentiation is not solely dependent on TGF-β1 but also on mechanical load through integrin signaling. These pathways may converge but also act in synergy. Therefore, a combination of phenotype conversion of MyoFb to nondifferentiated Fb through the TGF-β1 signaling path and cardiac unloading could hold promise as a therapeutic strategy. The recent data describing lack of fibrosis reduction with mechanical unloading could be interpreted as a requirement for targeting more than one pathway for treatment of fibrosis.

FIGURE 8 **Gene Expression Patterns in Treated HF Cells Are Reverting to Non-HF**

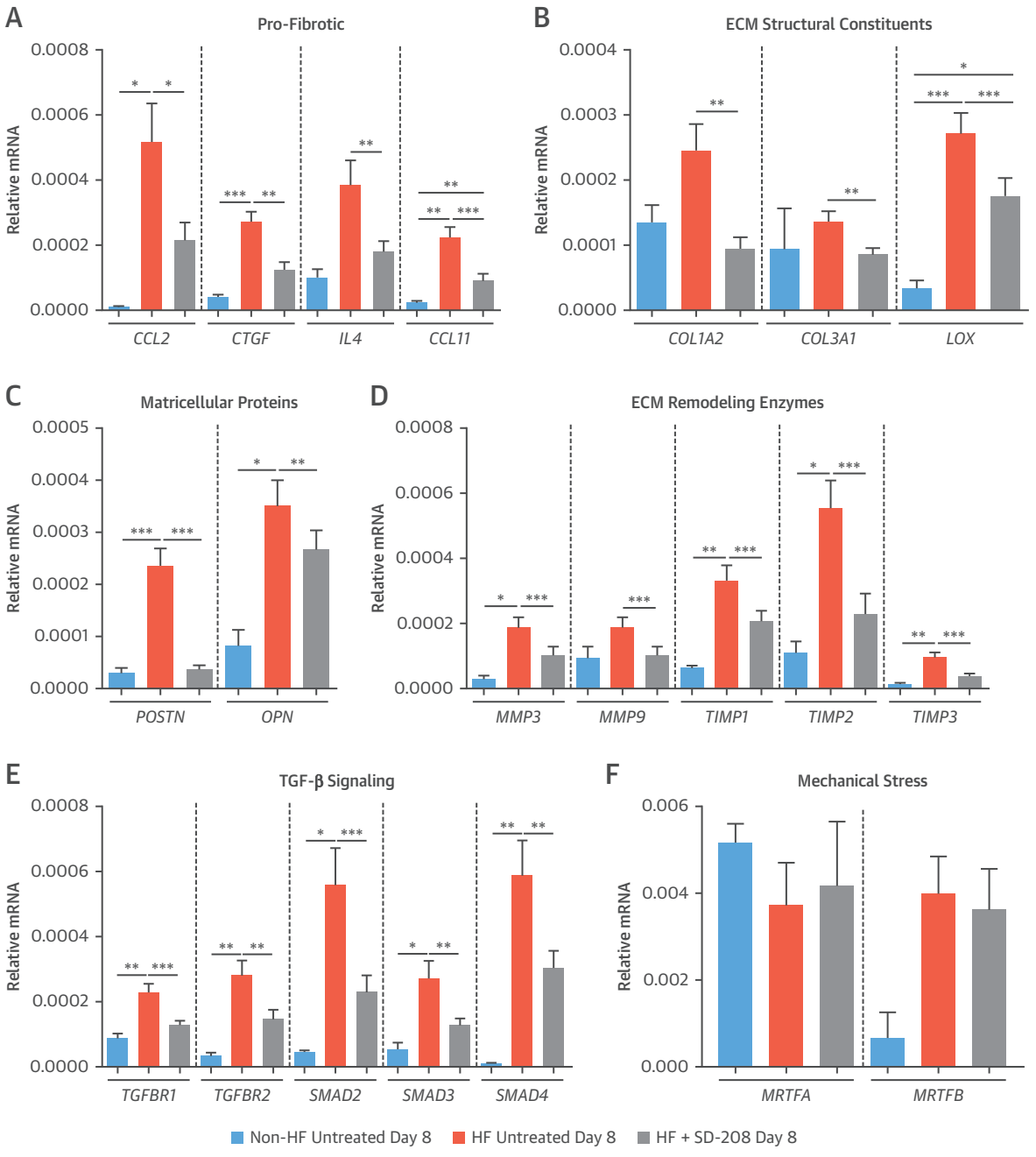

RT-qPCR performed on mRNA isolated from the same cell cultures phenotyped in Figure 5. **(A)** Pro-fibrotic genes *CCL2*, *CTGF*, *IL4*, and *CCL11*. **(B)** ECM constituent genes for collagen *COL1A2*, *COL3A1*, and *LOX*. **(C)** Genes for matricellular proteins: *POSTN* and *OPN*. **(D)** Genes for collagen turnover enzymes: *MMP3*, *MMP9*, *TIMP1*, *TIMP2*, and *TIMP3*. **(E)** TGF-beta signaling pathway genes *TGFBR1*, *TGFBR2*, *SMAD2*, *SMAD3*, and *SMAD4*. **(F)** Genes activated by mechanical stress, *MRTFA* and *MRTFB*. (Non-HF n = 3; HF hearts n = 9 and HF+SD-208 n = 9). *$p < 0.05$, **$p < 0.01$, ***$p < 0.001$ (1-way ANOVA with Bonferroni post hoc test). Abbreviations as in Figures 1, 2, and 3.

CENTRAL ILLUSTRATION **Heterogeneity of Fibroblasts in Heart Failure and Potential for Phenotype Reversibility**

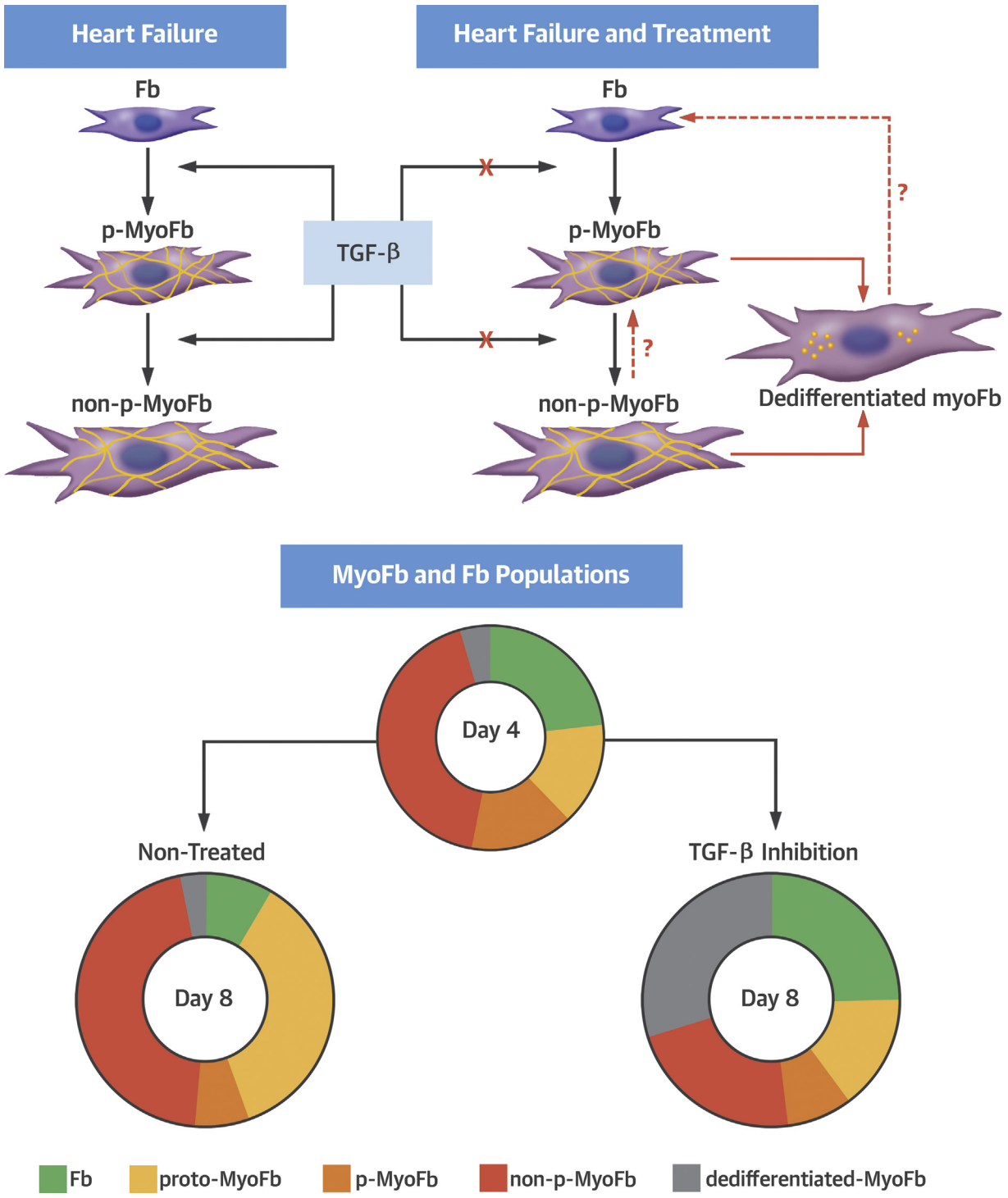

Nagaraju, C.K. et al. J Am Coll Cardiol. 2019;73(18):2267–82.

Fibroblastic cells isolated from HF hearts are mostly myofibroblasts (MyoFb), either still proliferating (proto-MyoFb or p-MyoFb) or not (non-p-MyoFb). Inhibition of TGF-β signaling for 4 days indicates that the majority of these cells retain the potential to dedifferentiate and/or revert to fibroblast phenotype. Fb = fibroblast; HF = heart failure; TGF = transforming growth factor.

STUDY LIMITATIONS. The study of human HF is limited by the scarcity of age-matched and disease-free control samples. The Non-HF samples come from hearts that were not suitable for transplantation for various reasons such as age, coronary artery lesions found on angiography, cardiac hypertrophy, high inotropic support in the donor, and suspected antecedents of hypertension. This implies that Non-HF used in the study may have moderate fibrosis, more than expected in the healthy population.

Although the biopsies used for histology, cell isolation, and molecular experiments came from the same hearts, regions within the LV could not always be matched precisely. In the ICM tissue samples, the biopsies were taken remote from the infarct zone, and presently, we have no data on scar tissue.

CONCLUSIONS

In advanced cardiac remodeling, MyoFb responsible for interstitial fibrosis retain the capacity for dedifferentiation. Small molecule targeting of signaling could open possibilities to reduce interstitial fibrosis even in advanced heart disease.

ACKNOWLEDGMENTS The authors thank Dr. Matthew Amoni and Dr. Jan Van Keer for their assistance during the heart sample collection, and the transplant team of UZ Leuven for help in providing human explanted hearts.

ADDRESS FOR CORRESPONDENCE: Dr. Karin R. Sipido, Department of Cardiovascular Sciences, Division of Experimental Cardiology, KU Leuven, Campus Gasthuisberg, Herestraat 49, B-3000 Leuven, Belgium. E-mail: karin.sipido@kuleuven.be. Twitter: @KU_Leuven.

PERSPECTIVES

COMPETENCY IN MEDICAL KNOWLEDGE: Cardiac MyoFb from patients with end-stage HF undergoing transplantation exhibit variable degrees of differentiation and retain the capacity to return to less activated states, indicating potential responsiveness to antifibrotic therapy.

TRANSLATIONAL OUTLOOK: Future studies using RNA sequencing technology may identify specific molecular pathways regulating MyoFb dedifferentiation as target to reverse fibrosis.

REFERENCES

1. Gourdie RG, Dimmeler S, Kohl P. Novel therapeutic strategies targeting fibroblasts and fibrosis in heart disease. Nat Rev Drug Discov 2016;15:620–38.

2. Kasner M, Westermann D, Lopez B, et al. Diastolic tissue Doppler indexes correlate with the degree of collagen expression and cross-linking in heart failure and normal ejection fraction. J Am Coll Cardiol 2011;57:977–85.

3. Westermann D, Lindner D, Kasner M, et al. Cardiac inflammation contributes to changes in the extracellular matrix in patients with heart failure and normal ejection fraction. Circ Heart Fail 2011;4:44–52.

4. Moore-Morris T, Guimarães-Camboa N, Banerjee I, et al. Resident fibroblast lineages mediate pressure overload-induced cardiac fibrosis. J Clin Invest 2014;124:2921–34.

5. Russo I, Frangogiannis NG. Diabetes-associated cardiac fibrosis: cellular effectors, molecular mechanisms and therapeutic opportunities. J Mol Cell Cardiol 2016;90:84–93.

6. Kawara T, Derksen R, de Groot JR, et al. Activation delay after premature stimulation in chronically diseased human myocardium relates to the architecture of interstitial fibrosis. Circulation 2001;104:3069–75.

7. Shinde A, Frangogiannis NG. Fibroblasts in myocardial infarction: a role in inflammation and repair. J Mol Cell Cardiol 2014;70:74–82.

8. Ruiz-Villalba A, Simón AM, Pogontke C, et al. Interacting resident epicardium-derived fibroblasts and recruited bone marrow cells form myocardial infarction scar. J Am Coll Cardiol 2015;65:2057–66.

9. Moore-Morris T, Cattaneo P, Guimarães-Camboa N, et al. Infarct fibroblasts do not derive from bone marrow lineages. Circ Res 2018;122:583–90.

10. Leask A. Getting to the heart of the matter: new insights into cardiac fibrosis. Circ Res 2015;116:1269–76.

11. Travers JG, Kamal FA, Robbins J, Yutzey KE, Blaxall BC. Cardiac fibrosis: the fibroblast awakens. Circ Res 2016;118:1021–40.

12. Moore L, Fan D, Basu R, Kandalam V, Kassiri Z. Tissue inhibitor of metalloproteinases (TIMPs) in heart failure. Heart Fail Rev 2012;17:693–706.

13. Spinale FG, Janicki JS, Zile MR. Membrane-associated matrix proteolysis and heart failure. Circ Res 2013;112:195–208.

14. Hermida N, López B, González A, et al. A synthetic peptide from transforming growth factor-β1 type III receptor prevents myocardial fibrosis in spontaneously hypertensive rats. Cardiovasc Res 2009;81:601–9.

15. Zhang Y, Elsik M, Edgley AJ, et al. A new anti-fibrotic drug attenuates cardiac remodeling and systolic dysfunction following experimental myocardial infarction. Int J Cardiol 2013;168:1174–85.

16. Travers JG, Kamal FA, Valiente-Alandi I, et al. Pharmacological and activated fibroblast targeting of Gβγ-GRK2 after myocardial ischemia attenuates heart failure progression. J Am Coll Cardiol 2017;70:958–71.

17. Hulsmans M, Sager HB, Roh JD, et al. Cardiac macrophages promote diastolic dysfunction. J Exp Med 2018;215:423–40.

18. López B, Querejeta R, Varo N, et al. Usefulness of serum carboxy-terminal propeptide of procollagen type I in assessment of the cardioreparative ability of antihypertensive treatment in hypertensive patients. Circulation 2001;104:286–91.

19. McMurray JJV, Adamopoulos S, Anker SD, et al. ESC guidelines for the diagnosis and treatment of acute and chronic heart failure 2012: the Task Force for the Diagnosis and Treatment of Acute and Chronic Heart Failure 2012 of the European Society of Cardiology. Eur J Heart Fail 2012;14:803–69.

20. Shimada YJ, Passeri JJ, Baggish AL, et al. Effects of losartan on left ventricular hypertrophy and fibrosis in patients with nonobstructive hypertrophic cardiomyopathy. J Am Coll Cardiol HF 2013;1:480–7.

21. Fairbairn TA, Steadman CD, Mather AN, et al. Assessment of valve haemodynamics, reverse ventricular remodelling and myocardial fibrosis following transcatheter aortic valve implantation compared to surgical aortic valve replacement: a cardiovascular magnetic resonance study. Heart 2013;99:1185–91.

22. Zafeiridis A, Jeevanandam V, Houser SR, Margulies KB. Regression of cellular hypertrophy after left ventricular assist device support. Circulation 1998;98:656–62.

23. Rodrigue-Way A, Burkhoff D, Geesaman BJ, et al. Sarcomeric genes involved in reverse remodeling of the heart during left ventricular assist device support. J Heart Lung Transplant 2005;24:73–80.

24. Slaughter MS, Rogers JG, Milano CA, et al. Advanced heart failure treated with continuous-flow left ventricular assist device. N Engl J Med 2009;361:2241–51.

25. Farris SD, Don C, Helterline D, et al. Cell-specific pathways supporting persistent fibrosis in heart failure. J Am Coll Cardiol 2017;70:344–54.

26. Velasquez LS, Sutherland LB, Liu Z, et al. Activation of MRTF-A-dependent gene expression with a small molecule promotes myofibroblast differentiation and wound healing. Proc Natl Acad Sci U S A 2013;110:16850–5.

27. Maruhashi T, Kii I, Saito M, Kudo A. Interaction between periostin and BMP-1 promotes proteolytic activation of lysyl oxidase. J Biol Chem 2010;285:13294–303.

28. Shinde AV, Humeres C, Frangogiannis NG. The role of α-smooth muscle actin in fibroblast-mediated matrix contraction and remodeling. Biochim Biophys Acta 2017;1863:298–309.

29. Riedl J, Crevenna AH, Kessenbrock K, et al. Lifeact: a versatile marker to visualize F-actin. Nat Methods 2008;5:605–7.

30. Beltrami CA, Finato N, Rocco M, et al. The cellular basis of dilated cardiomyopathy in humans. J Mol Cell Cardiol 1995;27:291–305.

31. Polyakova V, Loeffler I, Hein S, et al. Fibrosis in endstage human heart failure: severe changes in collagen metabolism and MMP/TIMP profiles. Int J Cardiol 2011;151:18–33.

32. Weber KT, Pick R, Janicki JS, Gadodia G, Lakier JB. Inadequate collagen tethers in dilated cardiopathy. Am Heart J 1988;116:1641–6.

33. Sager HB, Hulsmans M, Lavine KJ, et al. Proliferation and recruitment contribute to myocardial macrophage expansion in chronic heart failure. Circ Res 2016;119:853–64.

34. Galindo CL, Kasasbeh E, Murphy A, et al. Anti-remodeling and anti-fibrotic effects of the neuregulin-1β glial growth factor 2 in a large animal model of heart failure. J Am Heart Assoc 2014;3:e000773.

35. Hudson MP, Armstrong PW, Ruzyllo W, et al. Effects of selective matrix metalloproteinase inhibitor (PG-116800) to prevent ventricular remodeling after myocardial infarction: results of the PREMIER (Prevention of Myocardial Infarction Early Remodeling) trial. J Am Coll Cardiol 2006;48:15–20.

36. Ikeuchi M, Tsutsui H, Shiomi T, et al. Inhibition of TGF-beta signaling exacerbates early cardiac dysfunction but prevents late remodeling after infarction. Cardiovasc Res 2004;64:526–35.

37. Frantz S, Hu K, Adamek A, et al. Transforming growth factor beta inhibition increases mortality and left ventricular dilatation after myocardial infarction. Basic Res Cardiol 2008;103:485–92.

38. Driesen RB, Nagaraju CK, Abi-Char J, et al. Reversible and irreversible differentiation of cardiac fibroblasts. Cardiovasc Res 2014;101:411–22.

39. Beaumont J, López B, Hermida N, et al. microRNA-122 down-regulation may play a role in severe myocardial fibrosis in human aortic stenosis through TGF-β1 up-regulation. Clin Sci (Lond) 2014;126:497–506.

40. Tijsen AJ, Van Der Made I, Van Den Hoogenhof MM, et al. The microRNA-15 family inhibits the TGFβ-pathway in the heart. Cardiovasc Res 2014;104:61–71.

41. Flevaris P, Khan SS, Eren M, et al. PAI-1 controls cardiomyocyte TGF-β and cardiac fibrosis. Circulation 2017;136:664–79.

42. Kaur H, Takefuji M, Ngai CY, et al. Targeted ablation of periostin-expressing activated fibroblasts prevents adverse cardiac remodeling in mice. Circ Res 2016;118:1906–17.

43. Jeong D, Yang DK, Kho C, et al. Matricellular protein CCN5 reverses established cardiac fibrosis. J Am Coll Cardiol 2016;67:1556–68.

44. Schafer S, Viswanathan S, Widjaja AA, et al. IL-11 is a crucial determinant of cardiovascular fibrosis. Nature 2017;552:110–5.

45. Gladka MM, Molenaar B, de Ruiter H, et al. Single-cell sequencing of the healthy and diseased heart reveals cytoskeleton-associated protein 4 as a new modulator of fibroblasts activation. Circulation 2018;138:166–80.

KEY WORDS contractile function, extracellular matrix, fibroblasts, inflammation

APPENDIX For an expanded Methods section as well as supplemental figures and tables, please see the online version of this paper.